



Experimental evaluation of local wave speed in the presence of reflected waves



Alessandra Borlotti^{a,1}, Ye Li^{a,1}, Kim H. Parker^b, Ashraf W. Khir^{a,*}

^a Brunel Institute for Bioengineering, Brunel University, Uxbridge, Middlesex, UB8 3PH, UK

^b Department of Bioengineering, Imperial College London, London, UK

ARTICLE INFO

Article history:

Accepted 7 October 2013

Keywords:

Wave propagation
Local wave speed
Reflection waves
Flexible tubes
Reflection coefficient

ABSTRACT

Wave speed (also called pulse wave velocity) is the speed by which disturbance travels along the medium and it depends on the mechanical and geometrical properties of the vessel and on the density of the blood. Wave speed is a parameter of clinical relevance because it is an indicator of arterial stiffness and cardiovascular diseases.

The aim of this work is to compare different methods for the determination of local wave speed in bench experiments and investigate their relative accuracy when reflections are present.

Pressure (P), flow (Q) and diameter (D) were measured along a flexible tube far and close to three positive and three negative reflection sites. Wave speed was calculated using PU-loop, $(\ln D)U$ -loop, QA-loop, D^2P -loop, sum of squares and characteristic impedance methods. Results were compared to the foot-to-foot method.

We found that far from the reflections almost all methods give uniform results. Close to positive reflections the methods that rely on P and Q (or U) overestimate the wave speed value, while techniques based on D (or A) and Q (or U) underestimate it. On the contrary, close to negative reflections the methods that rely on P and Q (or U) underestimate the wave speed value, while techniques based on D (or A) and Q (or U) overestimate it. The D^2P -loop does not seem to be affected by positive or negative reflections.

Most of the methods currently used to determine local wave speed are affected by reflections, but the $(\ln D)U$ -loop remains the easiest technique to use in the clinic.

© 2013 Elsevier Ltd. All rights reserved.

1. Introduction

Wave speed (C), widely known by physiologists and clinicians as pulse wave velocity, is the speed by which disturbance travels along the medium (Lighthill, 1978). C depends on the mechanical and geometrical properties of the vessel, and on the density of the blood (Bramwell and Hill, 1922). That is why C is used as an indicator of arterial stiffness and cardiovascular risk (Blacher et al., 1999).

In current clinical practice the most commonly used method to calculate C is the foot-to-foot, which involves pressure measurements in two different sites at a known distance apart. This technique gives an average speed along the path traveled by the wave, often called regional C . The two measurements are usually taken at the carotid and femoral arteries with the resultant wave speed commonly known as the carotid-femoral index. However,

the carotid and femoral arteries have different mechanical properties, the former is an elastic and the latter is a muscular artery and they have different C (Borlotti et al., 2012). For this reason, regional C might not be an accurate parameter to determine the local arterial mechanical properties.

Local wave speed refers to the determination of C at a single measurement site; hence there can be clear prognostic value in determining local C . Several methods have been introduced to determine local C in arteries for diagnostic purpose. Westerhof et al. (1969) determined local C using Fourier-based frequency domain analysis, calculating the characteristic impedance (Z_C), which can be obtained from simultaneous measurements of pressure (P) and flow (Q) taken at the same site. More recently time-domain techniques were introduced for the determination of local C using two of the following simultaneous measurements: P , Q , velocity (U), diameter (D) and area (A). Khir et al. (2001) proposed the PU-loop method that relies on the linearity between P and U in the absence of reflections; the slope of the linear portion of the loop at early systole when most probably only forward waves are present indicates C . Rabben et al. (2004) introduced the QA-loop method that is based on the same principle

* Corresponding author. Tel.: +44 1895 265857; fax: +44 1895 274608.

E-mail address: Ashraf.khir@brunel.ac.uk (A.W. Khir).

¹ Authors contributed equally to the manuscript.

of the PU-loop. To accommodate the co-existence of incident and reflected waves in the coronary arteries, Davies et al. (2006) proposed the sum of squares technique deriving a formula that minimizes the net wave energy over a complete cardiac cycle using simultaneously P and U measurements. Feng and Khir (2010) introduced a technique that uses D and U measurements. Local wave speed is determined from the slope of the linear portion of the $(\ln D)U$ -loop in early systole and is equal to $1/2 C$. This method has the advantage that it does not rely on the invasive pressure measurement and uses D and U which can be easily acquired non-invasively in the superficial arteries. Alastruey (2011) proposed the D^2P -loop which relies on the determination of the slope of linear part of the loop in diastole assuming the arterial wall as Voigt-type visco-elastic material. The slope is equal to $D_0/\rho c^2$ (with D_0 , mean arterial diameter). All of the loop methods rely on the linear relationship between two measurements in a period that is reflection free where the wave speed can be calculated from the slope of the linear part of the loop; early systole for PU-loop, $(\ln D)U$ -loop and QA-loop, and late diastole D^2P -loop. If the measurement site is close to a reflection site the reflection-free period might be too short to allow for determining C accurately, as we previously demonstrated that the PU-loop method is affected by reflections (Li et al., 2011).

In this work we propose an experimental comparison of currently used methods for calculating local C in flexible tubes. The aim of this study is to investigate the relative accuracy of these methods for the determination of local wave speed compared to the foot-to-foot method. The aim is also, to establish the effect of positive and negative reflections on the results of these methods.

2. Material and methods

2.1. Theoretical background

In this section a brief description and the equations of all methods are reported.

2.1.1. Characteristic impedance (C_z)

Wave speed can be calculated using the characteristic Impedance (Z_c) as

$$C_z = \frac{AZ_c}{\rho} \quad (1)$$

where Z_c is calculated as the averaged ratio of P to Q moduli over a chosen frequency range (Westerhof et al., 1969, 1971, 1973; Milnor and Bertram, 1978).

In this work, we used four frequency ranges: 3–10 Hz, C_{z3-10} (Westerhof et al., 1973), 2–12 Hz, C_{z2-12} (Pepine et al., 1979), 5–15 Hz, C_{z5-15} (Dujardin et al., 1980), 9–18 Hz, C_{z9-18} (Cox and Bagshaw, 1975).

2.1.2. PU-loop (C_{pu})

This method assumes that in early systole backward waves are negligible, the relationship between P and U is linear and the wave speed can be calculated from the water-hammer equation as the slope of initial linear part of the loop

(Khir et al., 2001)

$$C_{pu} = \frac{1}{\rho} \frac{dP_{\pm}}{dU_{\pm}} \quad (2)$$

where dP and dU are the changes in pressure and velocity respectively, over the systolic initial linear range of the loop. ρ is fluid density and \pm indicate the forward and backward directions respectively.

2.1.3. Sum of squares (C_{pu}^{22})

This method was particularly introduced to avoid the reflections existing predominantly throughout the cardiac cycle in the coronary arteries. It is based on the minimization of the net wave energies over a cardiac cycle (Davies et al., 2006)

$$C_{p^2u^2} = \frac{1}{\rho} \sqrt{\frac{\sum (dP)^2}{\sum (dU)^2}} \quad (3)$$

2.1.4. QA-loop (C_{qa})

In the absence of reflected waves during early systole, C can be determined as (Rabben et al., 2004)

$$C_{qa} = \frac{dQ}{dA} \quad (4)$$

where dQ and dA are the changes in the flow rate and cross sectional area respectively, over the systolic linear range of the loop.

2.1.5. $(\ln D)U$ -loop (C_{du})

In the absence of reflected waves in early systole, the wave speed can be calculated as (Feng and Khir, 2010)

$$C_{du} = \frac{1}{2} \frac{dU_{\pm}}{d \ln D_{\pm}} \quad (5)$$

where $d \ln D$ is the change in logarithm the diameter over the systolic initial linear range of the loop.

2.1.6. D^2P -loop (C_{dp})

Considering the arterial wall as a Voigt-type viscoelastic material, during diastole the relationship between D^2 and P is nearly linear (Alastruey, 2011), and wave speed can be written as

$$C_{dp} = D_0 \sqrt{\frac{dP}{\rho d(D^2)}} \quad (6)$$

where D_0 is mean arterial diameter.

2.2. Experimental set-up

Pressure, flow and diameter were measured in a silicone tube, 10 mm diameter and 1 mm wall thickness, uniform along its 3 m length, which we called ‘mother’ tube (Fig. 1). Daughter tubes were connected to the mother tube to provide positive ($n=3$) and negative ($n=3$) reflection coefficients. The dimensions of the daughter tubes with the corresponding theoretical reflection coefficient (R_t) generated at the connection are reported in Table 1. R_t is calculated as

$$R_t = \frac{\frac{A_0 - A_1}{c_0} - \frac{A_1 - A_2}{c_1}}{\frac{A_0 - A_1}{c_0} + \frac{A_1 - A_2}{c_1}} \quad (7)$$

where 0 and 1 refer to up- and downstream the discontinuity, respectively. The mother tube was fully immersed into a water tank. The inlet and outlet of the tubes

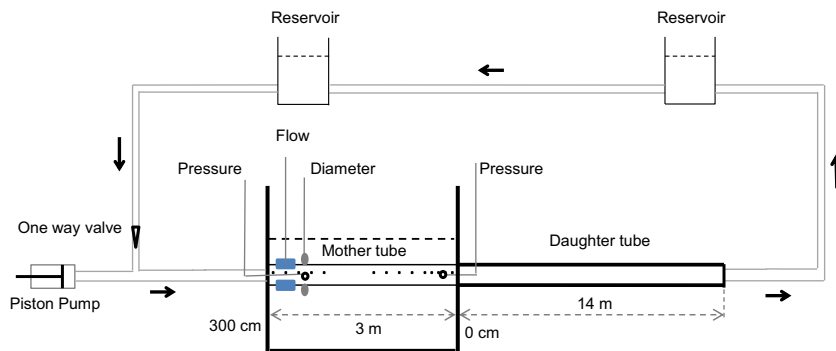


Fig. 1. Schematic representation of the experimental set-up. The arrows indicate the direction of flow. Dashed lines indicate level of fluid and the dots indicate the measurement sites.

were connected to reservoirs. The height of the fluid in the reservoirs was adjusted to 10 cm above the longitudinal axis of the tube in order to produce an initial hydrostatic pressure of 1 kPa. The inlet of the mother tube was connected to a piston pump, which produced an approximately semi-sinusoidal single pulse wave with a duration of approximately 0.26 s. P , Q and D waveforms were measured sequentially in time, every 10 cm along the mother tube and every 5 cm when the measurement site was 20 cm or less away from the reflection site (diameter measurements were not available in the last two positions for reflection coefficients R_4 and R_6). Due to the limited length of the pressure catheter, measurements could not be taken in the middle third of the mother tube. Wave speed calculated using the foot-to-foot method (C_{FTF}) was used as

Table 1
Dimensions and reflection coefficient of the daughter tubes.

| | D_{in} (mm) | h (mm) | Material | R_t |
|----|---------------|----------|----------|-------|
| R1 | 8 | 2 | Silicone | +0.36 |
| R2 | 8 | 1 | Silicone | +0.28 |
| R3 | 10 | 2 | Silicone | +0.12 |
| R4 | 12 | 1 | Silicone | -0.12 |
| R5 | 16.7 | 1.5 | Rubber | -0.39 |
| R6 | 21 | 1.5 | Rubber | -0.60 |

D_{in} is internal diameter, h is wall thickness and R_t is the theoretical reflection coefficient calculated using Eq. (8).

reference; another pressure transducer was placed at the end of the mother tube at known distance (285 cm) from the inlet of the mother tube and measurements were taken twice before each experiment. Pressure, flow and outer diameter were measured using an 8F tipped catheter pressure transducer (Millar Instruments Inc., Houston, USA), an ultrasonic flow probe (Transonic System, Inc, Ithaca, USA) and a paired set of ultrasonic crystals (Sonometrics Corporation, Ontario, Canada), respectively. The inner diameter, D , was determined by subtracting twice the wall thickness. All the data were sampled at 500 Hz using Sonolab (Sonometrics Corporation, London, Ontario, Canada). The analysis was carried out using programs written in Matlab (The Mathworks, Natick, MA, USA). A time delay of approximately 25 ms between the recorded signals due to the different frequency response of the measuring transducers was eliminated by aligning the signals using a previously described technique (Swalen and Khir, 2009). Then, the linear portion of the loops was determined by eye. Typical example of pressure, flow and diameter waveforms that were used to calculate the local wave speed with the different methods are shown in Fig. 2. A and U waveforms were calculated from D and Q measurements, as $\pi D^2/4$ and $4Q/\pi D^2$, respectively.

2.3. Analysis

At each measurement site wave speed was calculated using all the methods presented above. The value of wave speed in each position is the average of the two values obtained from the two measurements.

Wave speed calculated in the first meter of the tube (9 positions), where reflections probably do not affect the measurements, were averaged for each

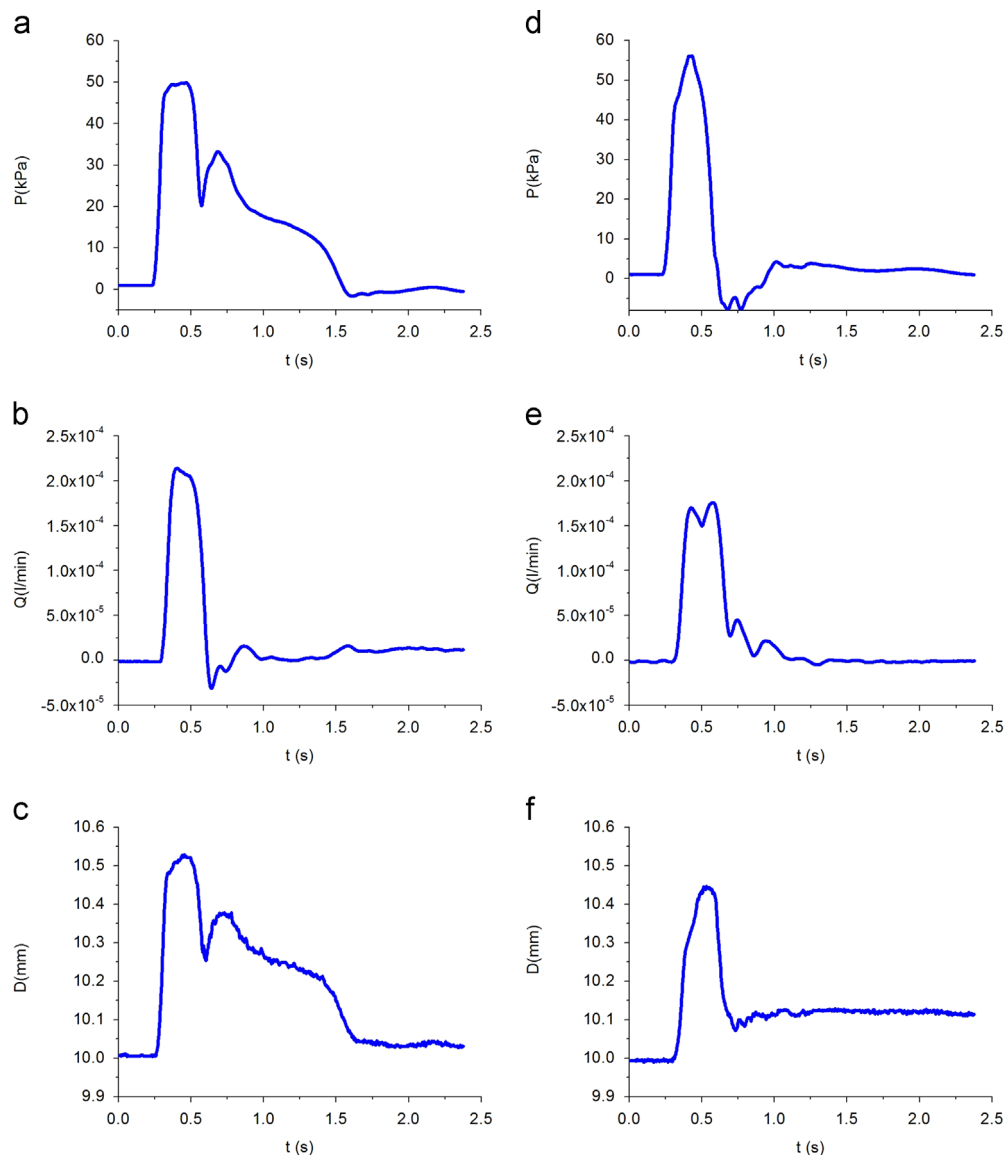


Fig. 2. Typical example of pressure (a) and (d), flow rate (b) and (e) and diameter (c) and (f) waveforms recorded in the mother tube with a positive reflection coefficient of +0.36 (left panel) and a negative reflection coefficient of -0.60 (right panel).

method and each reflection coefficient. The averaged value of C measured using each method at each measurement site ($n=9$) for all of the daughter tubes ($n=6$) was compared with the mean value of wave speed found using the foot-to-foot technique using a one-sample t -test. $p < 0.05$ were considered statistically significant.

In the last part of the tube (11 positions) percentage differences between the wave speed in each position calculated using each method and the foot-to-foot technique were calculated as $((C - C_{FTF})/C_{FTF}) \cdot 100$. Data in tables and figures are presented as mean value \pm SD.

3. Results

3.1. Wave speed in the reflection-free region

Figs. 3 and 4 show values of wave speed along the mother tube for all the reflection coefficients for the loops and sum of squares methods, and for the characteristic impedance technique, respectively.

We observe that in the reflection-free positions ($n=9$) in the first 100 cm from the inlet of the mother tube, all the methods, apart from C_{z9-18} , give similar results for both negative and positive reflections and the values are close to that determined using C_{FTF} . Table 2 includes the average values of wave speed over the first 9 positions for each reflection coefficient, where most probably reflections do not affect the results, for all the methods tested. We observe that the characteristic impedance has generally higher standard deviation compared to the loops and sum of squares methods. In particular, C_{pu} and C_{pu}^{22} have the lowest standard deviation and C_{z9-18} the highest.

3.2. Wave speed in the reflection-affected region

Wave speed measured at the last 100 cm away from the inlet of the mother tube, where reflections most probably affect the results,

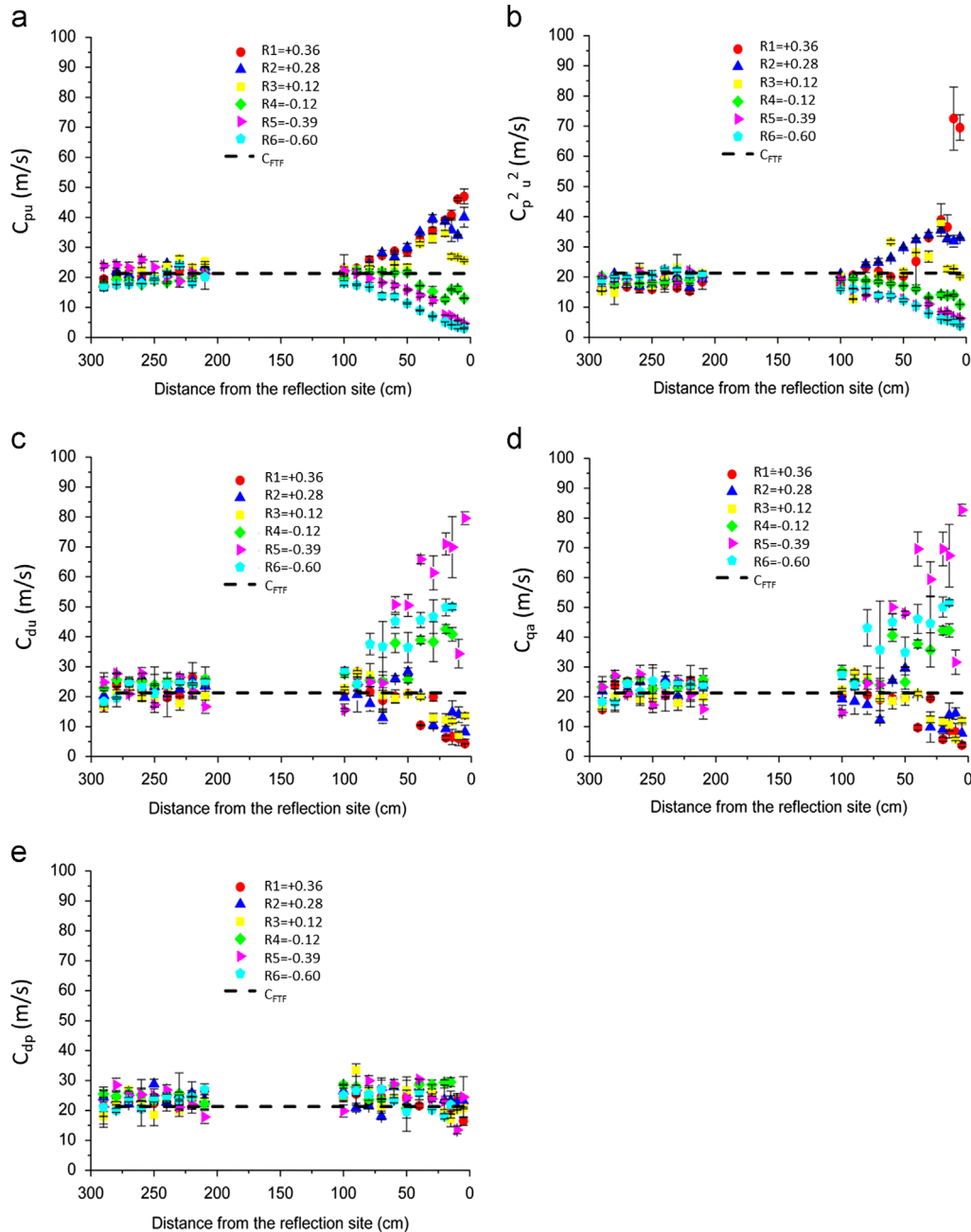


Fig. 3. Wave speed in all positions along the mother tube for all the reflection coefficients using: (a) PU-loop, (b) sum of squares (c) $(\ln D)U$ -loop, (d) QA-loop, (e) D^2P -loop. Positions 0 and 300 cm are the reflection site (positive or negative) and inlet of the mother tube, respectively. Each value is the average of two measurements. Dashed line is the value of wave speed calculated with the foot-to foot, $C_{FTF}=21.3$ m/s.

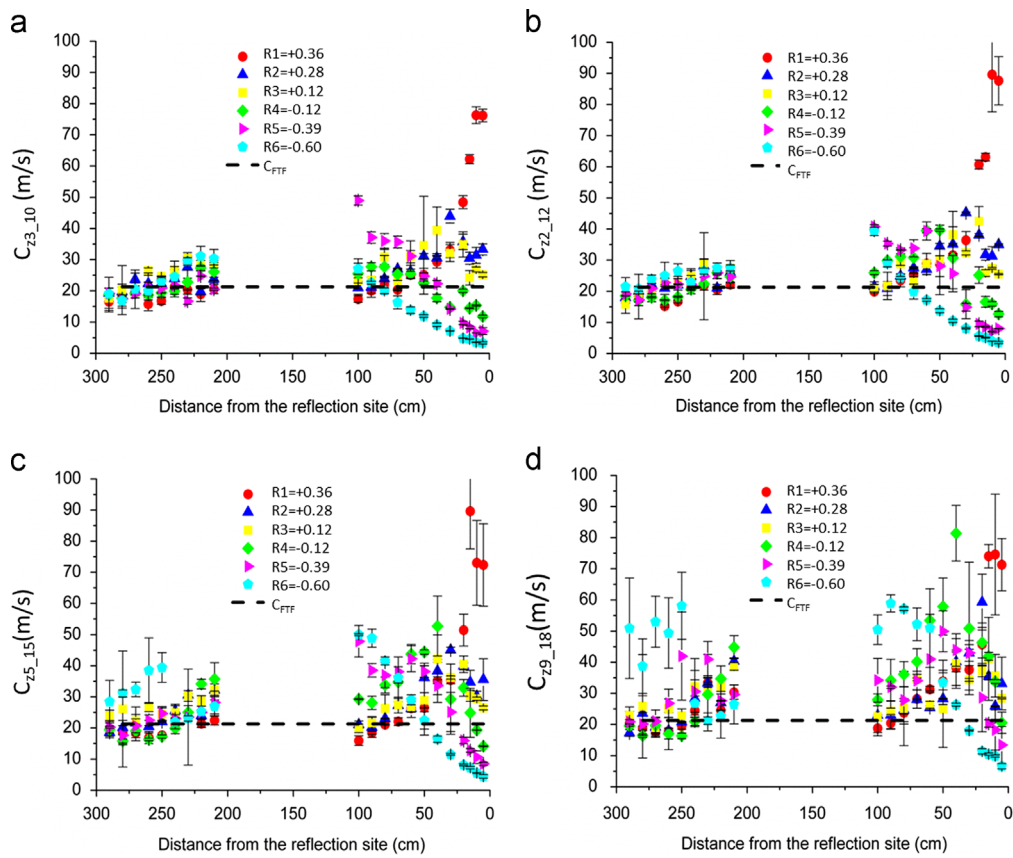


Fig. 4. Wave speed in all positions along the mother tube for all the reflection coefficients using: characteristic impedance with various frequency ranges as reported in the literature (a) 3–10 Hz, (b) 2–12 Hz, (c) 5–15 Hz and (d) 9–18 Hz. Positions 0 and 300 cm are the reflection site (positive or negative) and inlet of the mother tube, respectively. Each value is the average of two measurements. Dashed line is the value of wave speed calculated with the foot-to foot, C_{FTF} = 21.3 m/s.

Table 2

Averaged values of wave speed in the first meter of the mother tube calculated using the loops, sum of squares and the characteristic impedance methods. The characteristic impedance method is calculated using different range frequencies as reported in the literature.

| | R1 | R2 | R3 | R4 | R5 | R6 |
|---------------------|--------------|--------------|-------------|--------------|-------------|--------------|
| C_{pu} (m/s) | 20.6 ± 1.4 | 21.4 ± 2.4 | 22.1 ± 3.0 | 18.1 ± 1.0* | 22.5 ± 2.2 | 20.0 ± 1.1* |
| C_{du} (m/s) | 22.5 ± 3.1 | 23.1 ± 1.9* | 20.1 ± 1.0 | 24.6 ± 1.6** | 22.7 ± 4.3 | 22.8 ± 2.2 |
| C_{qa} (m/s) | 21.9 ± 3.2 | 23.0 ± 2.1* | 19.7 ± 1.8* | 24.5 ± 1.5** | 22.1 ± 4.1 | 22.7 ± 2.8 |
| C_{dp} (m/s) | 22.7 ± 1.7* | 24.4 ± 2.0** | 22.1 ± 2.8 | 24.6 ± 1.2** | 23.6 ± 3.3 | 23.2 ± 2.2* |
| C_{pu}^{22} (m/s) | 16.7 ± 0.9** | 18.4 ± 1.8** | 19.0 ± 3.0 | 18.8 ± 0.9** | 20.2 ± 1.4 | 20.6 ± 1.2 |
| C_{z3_10} (m/s) | 18.7 ± 2.0* | 22.4 ± 2.7 | 24.7 ± 4.5 | 21.1 ± 3.5 | 20.2 ± 2.4 | 23.8 ± 5.3 |
| C_{z2_12} (m/s) | 19.0 ± 2.5* | 22.5 ± 3.2 | 23.0 ± 4.4 | 20.3 ± 3.3 | 22.2 ± 2.8 | 24.6 ± 2.6* |
| C_{z5_15} (m/s) | 19.9 ± 2.2 | 23.9 ± 4.7 | 26.6 ± 3.2* | 22.5 ± 7.5 | 22.8 ± 3.1 | 29.7 ± 6.3** |
| C_{z9_18} (m/s) | 23.0 ± 5.7 | 25.3 ± 7.8 | 27.6 ± 6.1* | 24.3 ± 10.0 | 28.8 ± 8.1* | 38.6 ± 14.6* |

Values are mean ± SD.

* Indicates $p < 0.05$ compared to the mean value of the foot-to-foot technique that equals 21.3 m/s.

** Indicates $p < 0.001$ compared to the mean value of the foot-to-foot technique that equals 21.3 m/s.

is not uniform. Measured wave speed is increased or decreased exponentially than that calculated at the inlet of the tube.

For all positive reflection coefficients, C_{pu} , C_{pu}^{22} , C_{z3_10} , C_{z2_12} and C_{z5_15} , increased as the measurement site approached the reflection site, whereas C_{du} and C_{qa} decreased. C_{dp} does not seem to be affected by positive reflection. For all negative reflection coefficients, C_{pu} , C_z (ranges 3–10 Hz, 2–12 Hz, 5–15 Hz) and C_{pu}^{22} decreased as the measurement site approached the negative reflection site. Oppositely, C_{du} and C_{qa} increased. Also in this case we found that C_{dp} does not seem to be affected by reflections. Wave speed calculated using the characteristic impedance method

in the frequency range 9–18 Hz does not follow a specific pattern and overestimate wave speed with all the reflection coefficients.

3.3. Errors due to proximity to the reflection site

Figs. 5 and 6 show the percentage differences between the results of all the methods under investigation compared to C_{FTF} in the last 100 cm of the mother tube. The characteristic impedance methods show larger differences with C_{FTF} compared to the loops and sum of squares methods. The PU-loop and sum of squares methods show that the magnitude of the error in wave speed at

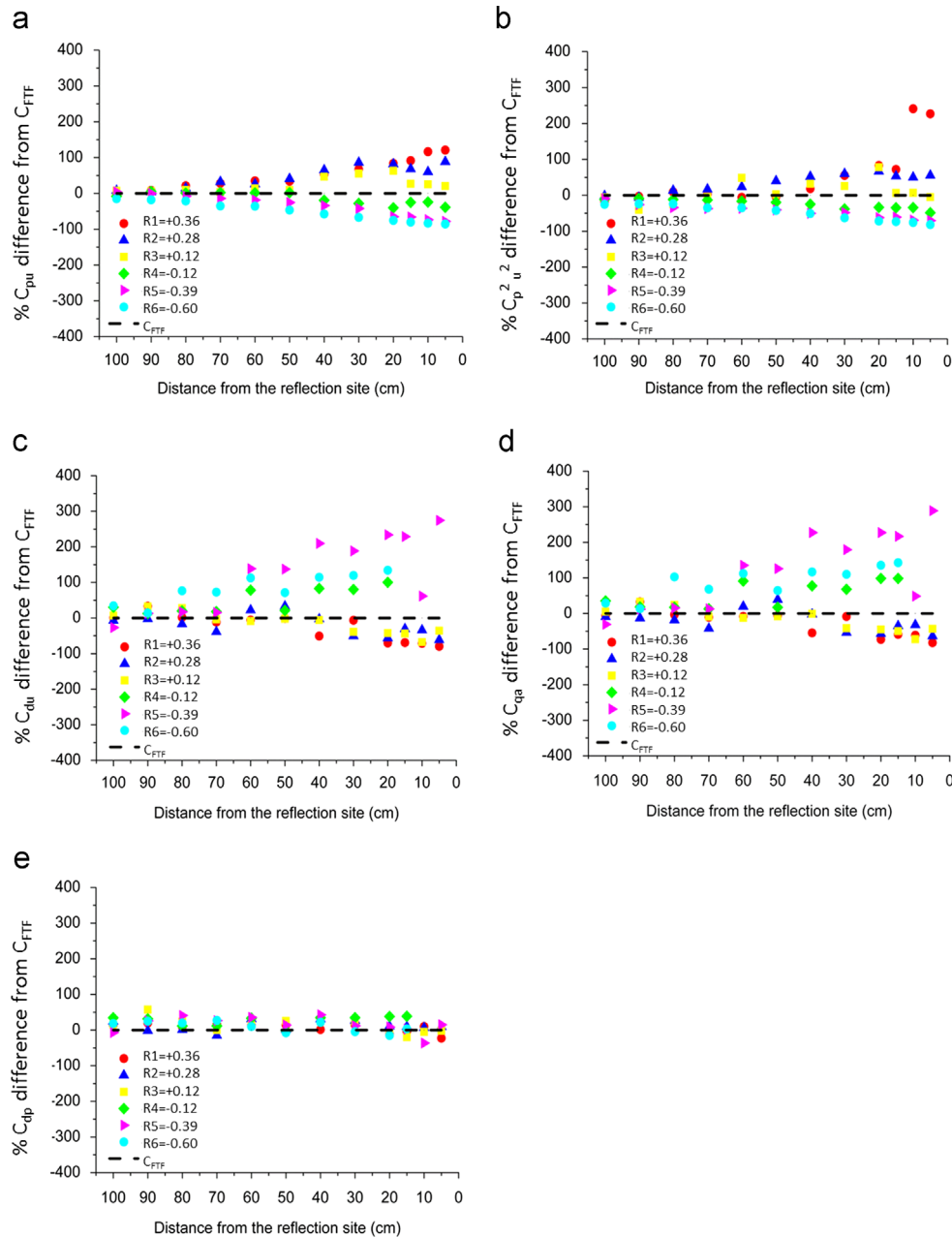


Fig. 5. Percentage differences of wave speed in the 11 positions closest to the reflection site and the wave speed calculated using the foot-to-foot technique (dashed line) using: (a) PU-loop, (b) sum of squares (c) (lnD)U-loop, (d) QA-loop, (e) D^2P -loop. Percentage differences were calculated as $((C - C_{FTF})/C_{FTF}) \cdot 100$.

a fixed distance from the reflection site increased with increasing value of reflection coefficient, more than the other techniques, where this behavior is less evident.

4. Discussion

Wave speed is a hemodynamic parameter that is directly related to arterial stiffness, and has been used as an indicator of cardiovascular events and mortality (Laurent et al. 2001). Further, methods used for the separation of waves into their forward and backward direction require an estimate of wave speed. In particular, wave speed is required in using wave intensity analysis for the determination of magnitude of the reflected wave and reflection indices. A useful meta-analysis by Baksi et al. (2009) on wave reflection highlighted the time of arrival of reflected waves in systole, and thus the importance wave speed in its calculations.

However, an accurate determination of local wave speed in human is still challenging due to the complexity of the arterial network that causes the forward wave to be reflected from multiple proximal small reflection sites rather than from discrete reflections located at the periphery (Davies et al., 2012). Although, it seems that reflections in the ascending aorta are relatively small even during occlusions (Borlotti and Khir, 2011) and they are not the major determinant of the central blood pressure waveform shape (Davies et al., 2010; Schultz et al., 2013), the phenomenon of reflection is the main obstacle for an accurate determination of wave speed using methods that rely on a reflection-free period.

In this study, we investigated the effect of positive ($n=3$) and negative ($n=3$) reflection coefficients on local wave speed as determined by the loops ($n=4$), sum of squares, and characteristic impedance ($n=4$) methods. All the results were compared to the wave speed determined using the foot-to-foot method, C_{FTF} , as the gold standard. The results indicate that, wave speed measured

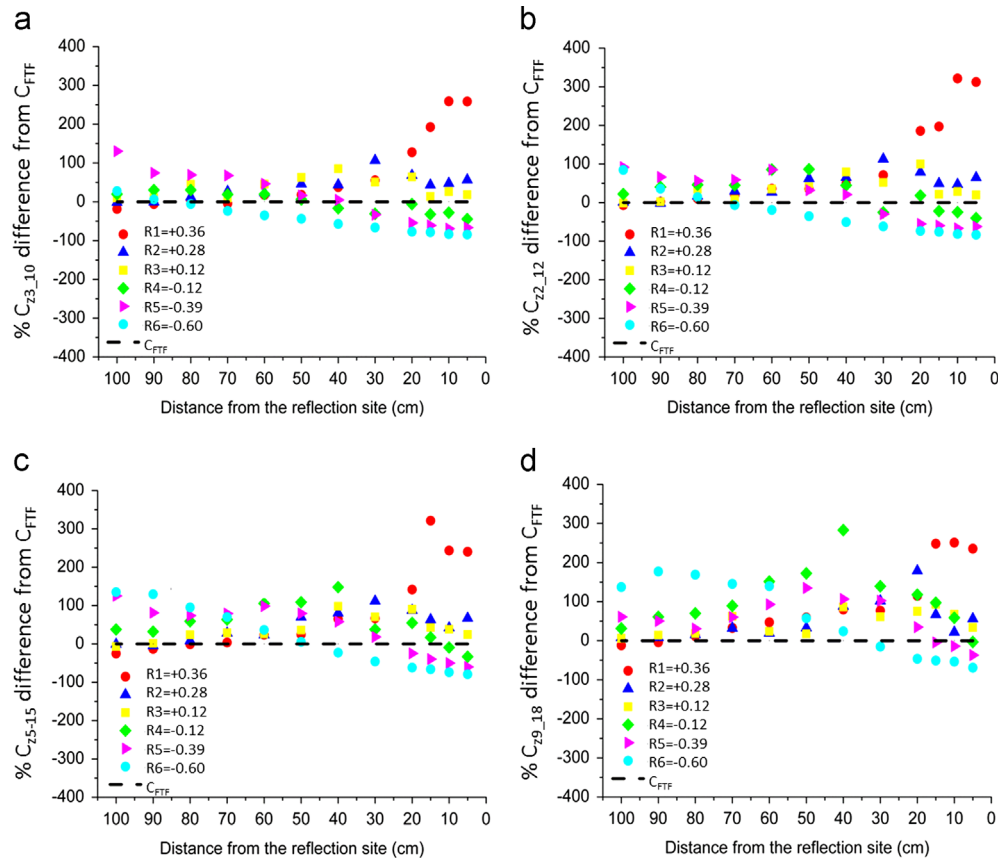


Fig. 6. Percentage differences of wave speed in the 11 positions closest to the reflection site and the wave speed calculated using the foot-to-foot technique (dashed line) using characteristic impedance method with various frequency ranges as reported in the literature: (a) range 3–10 Hz, (b) 2–12 Hz, (c) 5–15 Hz and (d) 9–18 Hz. Percentage differences were calculated as $((C - C_{FTF})/C_{FTF}) \cdot 100$.

close to the reflection site using methods based on P and U ; C_{pu} and C_{pu}^{22} , have similar error trends (Fig. 3a and b). Also, techniques based on D and U , and Q and A ; C_{du} and C_{qa} have similar trends (Fig. 3c and d), but in the opposite direction to P and U based methods.

In the first 100 cm of the mother tube all methods, a part from C_{z9-18} , yield uniform results even if in some cases the averaged value of wave speed is statistically different from that calculated using the foot-to-foot technique (Table 2). Whilst C_{pu}^{22} method systematically gives slightly lower wave speed compared to C_{FTF} , $(\ln D)U$ -loop, QA-loop and D^2P -loop yield higher values. In the last meter of the mother tube, all methods, are affected by reflections with the exception of the D^2P -loop that gives uniform results also in this part. We found that C_{pu} , C_{pu}^{22} and C_z increased and decreased as the measurement site became closer to the positive and negative reflection sites respectively. Oppositely C_{du} and C_{qa} decreased and increased as the measurement site approached the positive and negative reflection sites respectively. The differences from the foot-to-foot technique increased with proximity to the reflection site probably because of the increased size of the reflected wave.

By definition, a backward compression wave results in an increase of P and D (or A) and a decrease of U (or Q). This indicates that in the presence of positive reflections, methods using Eqs. (1)–(3) are expected to produce an error (increase) in the measurement of C . Oppositely, a backward expansion wave results in an increase of U (or Q) and decrease in P and D (or A), which results in an error (decrease) in the measurement of C . The results presented in Figs. 3 and 4 agree well with these theoretical considerations. Since the effect of backward waves on P and D have the same trend, this could produce a cancelling effect that

results in a correct estimation of wave speed. C_{dp} does not seem to be affected by reflections whether it is positive or negative; the averaged wave speed close to the positive reflections (36 positions) is 23.4 ± 3.5 m/s and close to negative reflections (32 positions) is 24.9 ± 4.0 m/s. However, this method seems to overestimate the value of wave speed.

The determination of the wave speed using the PU-loop in proximity of a reflection site, with the existence of a prominent reflected wave, has been investigated in our previous work (Li et al., 2011). We found that in the presence of positive and negative reflections, the PU-loop respectively over- and underestimates C . Our previous and current results agree with those recently reported by (Swillens et al., 2013) who compared the PU-loop, $(\ln D)U$ -loop and QA-loop in a computational model of the human carotid artery and in a population of healthy subjects. These findings could support the results of our previous work (Borlotti et al., 2012), where C_{du} determined at the carotid artery was lower than those calculated in the same population using pressure and distensibility (Vermeersch et al., 2008).

Although there is not yet available a gold standard method for the local determination of C in the presence of reflection, measurements in human arteries appear reliable (Zambanini et al., 2005; Davies et al., 2006; Curtis et al., 2007). This can be explained in two ways; (a) the measurements were taken far enough from the closest reflection site and (b) the magnitude of the reflection was very small, that it does not affect the measurements. This is not surprising if we consider that the arterial network is well matched in the forward direction (Gosling et al., 1971; Papageorgiou et al., 1990). This means that the reflection coefficients at bifurcations are very small, thus the wave speed error might be negligible even if the measurement is taken close to the

reflection site. But with age and cardiovascular diseases, reflection coefficients of bifurcation might increase leading to larger errors in the wave speed determination.

A computational comparison between all of the time-domain methods in a 1D model of the arterial system was recently conducted (Alastruey, 2011). The author concluded that C calculated using the loop methods were closer to theoretical values and more uniform within each arterial segment than those obtained using the sum of squares. He also reported that the D^2P -loop method led to the smallest differences with the theoretical value, calculated from the tube law (Eq. (2) in Alastruey, 2011).

The classical Moens–Kortweg equation (Kortweg, 1878; Moens, 1879), $c = \sqrt{Eh/\rho D}$, where E is the Young's modulus of the tube and h is the wall thickness, will not be affected by reflections. This is because it relies on measurements of mechanical properties of the wall and not the hemodynamic parameters. Whilst this is certainly an advantage, measurements of Young's modulus and wall thickness in vivo noninvasively, may not be possible. Therefore we believe that although affected by reflections similar to other the techniques, the $(\ln D)U$ -loop method remains the easiest to use in the clinic due to the availability of ultrasound technology to record both velocity and diameter.

4.1. Experimental considerations

The D^2P -loop technique introduced by (Alastruey, 2011), C_{dp} was determined in the diastolic part of the cardiac cycle where the relationship between D^2 and P was linear. In the waveforms of our experiments it was more difficult to detect the linear part of the loop at the end of the pulse, and therefore C_{dp} has been computed from the initial linear portion—this remains valid as it follows the same concept of establishing the slope of a linear portion of the loop in the absence of reflections.

The length of the mother tube was needed to ensure that the reflected wave generated at the end of the interface with each daughter tube arrives at the inlet of the mother tube after the incident wave has passed. Each daughter tube was 14 m long, which was also needed to ensure that measurements taken nearer the end of the mother tube are affected only by the reflected wave that is generated at the interface with the daughter tube; the reflected wave generated at the end of the daughter tubes arrives after the incident wave has passed even nearer the outlet of the mother tube.

5. Conclusion

Local wave speed measured using the PU-loop, $(\ln D)U$ -loop, QA-loop, sum of squares and characteristic impedance are affected by both negative and positive reflections. The D^2P -loop does not seem to be affected by reflection but the $(\ln D)U$ -loop remains the easiest technique to use in clinic. Methods based on the characteristic impedance technique show a higher variability compared to the loops and sum of squares methods. Methods that rely on pressure and velocity (or flow) over- and underestimate wave speed when in the presence of positive and negative reflections, respectively. On the contrary, methods that rely on diameter (or area) and velocity (or flow) over- and underestimate wave speed in the presence of negative reflection and positive reflections, respectively. To improve the reliability of the methods investigated in this work, the development of a correction algorithm is required to account for the errors introduced by reflections.

Conflict of interest statement

There is no conflict of interest between the authors of this paper and other external researchers or organisations that could have inappropriately influenced this work.

Acknowledgments

A. Borlotti holds the Isambard Research Scholarship offered by Brunel University, which the authors gratefully acknowledge.

References

- Alastruey, J., 2011. Numerical assessment of time-domain methods for the estimation of local arterial pulse wave speed. *J. Biomech.* 44 (5), 885–891.
- Baksi, A.J., Treibel, T.A., Davies, J.E., Hadjiloizou, N., Foale, R.A., Parker, K.H., Francis, D.P., Mayet, J., Hughes, A.D., 2009. A meta-analysis of the mechanism of blood pressure change with aging. *J. Am. Coll. Cardiol.* 54 (22), 2087–2092.
- Blacher, J., Asmar, R., Djane, S., London, G., Safar, M., 1999. Aortic pulse wave velocity as a marker of cardiovascular risk in hypertensive patients. *Hypertension* 33, 1111–1117.
- Borlotti, A., Khir, A.W., 2011. Wave speed and intensity in the canine aorta: analysis with and without the Windkessel-wave system. In: *Engineering in Medicine and Biology Society, EMBC, 2011 Annual International Conference of the IEEE* pp. 219–222.
- Borlotti, A., Khir, A.W., Rietzschel, E.R., De Buyzere, M.L., Vermeersch, Segers, P., 2012. Non-invasive determination of local pulse wave velocity and wave intensity: changes with age and gender in the carotid and femoral arteries of healthy human. *J. Appl. Physiol.* 113 (5), 727–735.
- Bramwell, J.C., Hill, A.V., 1922. The velocity of the pulse wave in man. *Proc. R. Soc. London, Ser. B*, 298–306.
- Cox, R.H., Bagshaw, R.J., 1975. Baroreceptor reflex control of arterial hemodynamics in the dog. *Circ. Res.* 37, 772–786.
- Curtis, S.L., Zambanini, A., Mayet, J., Thom, S.A.M., Foale, R., Parker, K.H., Hughes, A.D., 2007. Reduced systolic wave generation and increased peripheral wave reflection in chronic heart failure. *Am. J. Physiol.—Heart Circ. Physiol.* 293 (1), H557–H562.
- Davies, J.E., Whinnett, Z.I., Francis, D.P., Willson, K., Foale, R.A., Malik, I.S., Hughes, A.D., Parker, K.H., Mayet, J., 2006. Use of simultaneous pressure and velocity measurements to estimate arterial wave speed at a single site in humans. *Am. J. Physiol.—Heart Circ. Physiol.* 290 (2), H878–H885.
- Davies, J.E., Baksi, A.J., Francis, D.P., Hadjiloizou, N., Whinnett, Z.I., Manisty, C.H., Aguado-Sierra, J., Foale, R.A., et al., 2010. The arterial reservoir pressure increases with aging and is the major determinant of the aortic augmentation index. *Am. J. Physiol.—Heart Circ. Physiol.* 298 (2), H580–H586.
- Davies, J.E., Alastruey, J., Francis, D.P., Hadjiloizou, N., Whinnett, Z.I., Manisty, C.H., Aguado-Sierra, J., Willson, K., et al., 2012. Attenuation of wave reflection by wave entrapment creates a “horizon effect” in the human aorta. *Hypertension* 60 (3), 778–785.
- Dujardin, J.P., Stone, D.N., Paul, L.T., Pieper, H.P., 1980. Response of systemic arterial input impedance to volume expansion and hemorrhage. *Am. J. Physiol.—Heart Circ. Physiol.* 238 (7), H902–H908.
- Feng, J., Khir, A.W., 2010. Determination of wave speed and wave separation in the arteries using diameter and velocity. *J. Biomech.* 43 (3), 455–462.
- Gosling, R.G., Newman, D.L., Bowden, N.L., Twinn, K.W., 1971. The area ratio of normal aortic junctions. Aortic configuration and pulse-wave reflection. *Br. J. Radiol.* 44 (527), 850–853.
- Khir, A.W., O'Brien, A., Gibbs, J.S.R., Parker, K.H., 2001. Determination of wave speed and wave separation in the arteries. *J. Biomech.* 34 (9), 1145–1155.
- Kortweg, D.J., 1878. Ueber die Fortpflanzungsgeschwindigkeit des Schalles in elastischen Röhren. *Ann. Phys.* 241 (12), 525–542.
- Laurent, S., Boutouyrie, P., Asmar, R., Gautier, I., Laloux, B., Guize, L., Ducimetiere, P., Benetos, A., 2001. Aortic stiffness is an independent predictor of all-cause and cardiovascular mortality in hypertensive patients. *Hypertension* 37 (5), 1236–1241.
- Li, Y., Borlotti, A., Parker, K.H., Khir, A.W., 2011. Variation of wave speed determined by the PU-loop with proximity to a reflection site. In: *Proceedings of the Annual International Conference of the IEEE Engineering in Medicine and Biology Society*. Boston, pp. 199–202.
- Lighthill, J., 1978. *Waves in Fluids*. Cambridge University Press, Cambridge.
- Milnor, W.R., Bertram, C.D., 1978. The relation between arterial viscoelasticity and wave propagation in the canine femoral artery in vivo. *Circ. Res.* 43 (6), 870–879.
- Moens, A.L., 1879. Der erste Wellengipfel in dem absteigenden Schenkel der Pulscurve. *Pflüger, Archiv für die Gesamte Physiologie des Menschen und der Thiere* 20 (1), 517–533.
- Papageorgiou, G.L., Jones, B.N., Redding, V.J., Hudson, N., 1990. The area ratio of normal arterial junctions and its implications in pulse wave reflections. *Cardiovasc. Res.* 24 (6), 478–484.
- Pepine, C.J., Nichols, W.W., Curry Jr., R.C., Conti, R.C., 1979. Aortic input impedance during nitroprusside infusion. *Eur. J. Clin. Invest.* 64, 643–654.

- Rabben, S.I., Stergiopoulos, N., Hellevik, L.R., Smiseth, O.A., Slordahl, S., Urheim, S., Angelsen, B., 2004. An ultrasound-based method for determining pulse wave velocity in superficial arteries. *J. Biomech.* 37 (10), 1615–1622.
- Schultz, M.G., Davies, J.E., Roberts-Thomson, P., Black, J.A., Hughes, A.D., Sharman, J.E., 2013. Exercise central (Aortic) blood pressure is predominantly driven by forward traveling waves, not wave reflection. *Hypertension* 62 (1), 175–182.
- Swalen, M.J.P., Khir, A.W., 2009. Resolving the time lag between pressure and flow for the determination of local wave speed in elastic tubes and arteries. *J. Biomech.* 42 (10), 1574–1577.
- Swillens, A., Taelman, L., Degroote, J., Vierendeels, J., Segers, P., 2013. Comparison of non-invasive methods for measurement of local pulse wave velocity using FSI-simulations and in vivo data. *Ann. Biomed.* 41 (7), 1567–1578.
- Vermeersch, S.J., Rietzschel, E.R., De Buyzere, M.L., De Bacquer, D., De Backer, G., Van Bortel, L.M., Gillebert, T.C., Verdonck, P.R., Segers, P., 2008. Age and gender related patterns in carotid-femoral PWV and carotid and femoral stiffness in a large healthy, middle-aged population. *J. Hypertens.* 26 (7), 1411–1419.
- Westerhof, N., Bosman, F., De Vries, C.J., Noordergraaf, A., 1969. Analog studies of the human systemic arterial tree. *J. Biomech.* 2 (2), 121–134. (IN1, 135–136, IN3, 137–138, IN5, 139–143.)
- Westerhof, N., Elzinga, G., Sipkema, P., 1971. An artificial arterial system for pumping hearts. *J. Appl. Physiol.* 31 (5), 776–781.
- Westerhof, N., Elzinga, G., Van Den Bos, G.C., 1973. Influence of central and peripheral changes on the hydraulic input impedance of the systemic arterial tree. *Med. Biol. Eng.* 11 (6), 710–723.
- Zambanini, A., Cunningham, S.L., Parker, K.H., Khir, A.W., Thom, S.A.M., Hughes, A.D., 2005. Wave-energy patterns in carotid, brachial, and radial arteries: a noninvasive approach using wave-intensity analysis. *Am. J. Physiol.—Heart Circ. Physiol.* 289 (1), H270–H276.